Journal of Cleaner Production 572 (2026) 148908

Contents lists available at ScienceDirect

Journal of Cleaner Production

journal homepage: www.elsevier.com/locate/jclepro

A field-scale model using an integrated framework for evaluating food and water dynamics in agrivoltaics in three-dimensional space

Anh H. Nguyen [a], Yaoze Liu [a,*], Siyu Li [a], Zhuohang Wu [a], Majdi R. Abou Najm [b], Liming Zhou [c], Xiaobo Xue Romeiko [d], Richard R. Perez [e], Mark E. Uchanski [f], Jennifer M. Bousselot [f], Hu Liu [g], Chuandong Wu [h]

[a] *Department of Environmental and Sustainable Engineering, University at Albany, State University of New York, Albany, NY, 12222, USA*
[b] *Department of Land, Air and Water Resources, University of California, Davis, CA, 95616, USA*
[c] *Department of Atmospheric and Environmental Sciences, University at Albany, State University of New York, Albany, NY, 12222, USA*
[d] *Department of Environmental Health Sciences, University at Albany, State University of New York, Rensselaer, NY, 12144, USA*
[e] *Atmospheric Sciences Research Center, University at Albany, State University of New York, Albany, NY, 12222, USA*
[f] *Department of Horticulture and Landscape Architecture, Colorado State University, Fort Collins, CO, 80523, USA*
[g] *Northwest Institute of Eco-Environment and Resources, Chinese Academy of Sciences, Lanzhou, 730000, China*
[h] *State Key Laboratory of Hydroscience and Engineering, Department of Hydraulic Engineering, Tsinghua University, Beijing, 100084, China*

ARTICLE INFO

Keywords:
Agrivoltaics
Soil
Plant
Water
Biomass
Evapotranspiration

ABSTRACT

Growing pressure on food production, water resources, and renewable energy deployment has increased the need for integrated land-use strategies. Agrivoltaic systems (AVS), which co-locate solar photovoltaic (PV) installations with agricultural production, have emerged as a promising solution to improve land-use efficiency and climate resilience. However, existing modelling approaches are limited in their ability to represent the three-dimensional interactions governing food and water dynamics within AVS environments. This study developed a field-scale model (AVS-FW) using an integrated framework to represent the key factors affecting food and water dynamics in AVS in three-dimensional space. The AVS-FW used the framework to integrate the AVS-Microclimate model (simulating three-dimensional microclimatic conditions under solar panels), R-SWMS model (simulating three-dimensional soil condition and water transport), and Soil and Water Assessment Tool (SWAT) crop growth module (simulating plant growth). The AVS-FW model was demonstrated on a site in Colorado, USA, through scenario-based simulations comparing conditions with and without solar PV panels. The average actual evapotranspiration, water stored at the root depth, and biomass of lettuce with solar panels compared to without solar panels changed by −2.43% to −26.28%, 0.80% to 10.63%, and −3.17% to −34.63%, respectively. The temporal patterns of cumulative fluxes across soil domain boundaries were similar for cases with/without solar panels, but their magnitudes varied; and these were also found for total water volume in soil domain. The framework of the AVS-FW can assist decision-makers in evaluating the impacts of varied layouts (azimuth angles, inclinations, spacing, heights) and dimensions (lengths/widths) of solar PV panels on food and water dynamics in AVS.

1. Introduction

Global demand for both energy and food is expected to rise sharply as a result of population growth and continued economic development (Hassanpour Adeh et al., 2018; A. Nguyen et al., 2022). These pressures have accelerated international efforts to advance renewable energy technologies and improve agricultural sustainability. According to the International Energy Agency (IEA, 2025), global renewable capacity additions reached record levels in recent years, with solar photovoltaic (PV) being the fastest-growing technology with the total installed PV capacity reaching approximately 2.2 TW (TW) worldwide in 2024, accounting for the largest share of renewable expansion. Likewise, the International Renewable Energy Agency (IRENA) reports that renewables represented more than 90% of global power capacity expansion, highlighting the rapid global transition toward solar energy technologies (IRENA, 2025). At the same time, enhancing agricultural

* Corresponding author.
E-mail address: yliu46@albany.edu (Y. Liu).

https://doi.org/10.1016/j.jclepro.2026.148908
Received 14 November 2025; Received in revised form 29 June 2026; Accepted 4 July 2026
Available online 6 July 2026

productivity and improving land-use efficiency remain critical to ensure food security. Food and Agriculture Organization (FAO), however, highlights that agriculture accounts for about 70% of global freshwater withdrawals, placing increasing pressure on water resources (FAO, 2021). While utility-scale PV solar installations represent one of the most effective strategies for meeting expanding energy requirements, large-scale deployment of PV systems demands extensive land resources, often creating competition with agricultural uses (Hassanpour Adeh et al., 2018). Water availability further complicates this challenge, as irrigated farming depends heavily on reliable supplies that are increasingly threatened by scarcity and depletion. Consequently, balancing solar energy development, food production, and water management within the Food-Energy-Water (FEW) nexus has emerged as a central challenge for achieving sustainable development.

Agrivoltaic systems (AVS), which integrate solar PV infrastructure with cropland within agro-ecosystems, are a sustainable strategy for simultaneously addressing challenges of food security, water management, and renewable energy generation (Campana et al., 2021; Turnley et al., 2024; Varo-Martínez et al., 2024; L. Zhang et al., 2025). By harnessing solar energy directly on agricultural land or insect net house (Gadhiya et al., 2024), AVS offer a pathway to enhance land-use efficiency and pest management, while fostering synergistic interactions between crop cultivation and energy production (Pourshafi et al., 2025). The placement of PV panels above crops enables the generation of clean electricity while also creating shaded microclimates that can improve growing conditions and increase agricultural yields in certain contexts. This dual-use configuration mitigates competition for land resources by promoting coexistence and mutual benefits between farming and energy systems (Campana et al., 2021; Turnley et al., 2024; Varo-Martínez et al., 2024; L. Zhang et al., 2025). A review concludes that AVS offer “tangible potential”, especially in moderate climates (Pekk et al., 2025). Market analyses forecast the sector's global PV share's growth by about 50% over the next decade, reaching a cumulative value in the tens of billions U.S. dollars (Mahim et al., 2026). An assessment shows that AVS on just 1% of European Union's utilized agricultural area could yield 315-1415 GW, while the 2030 goal of 800 GW would require less than 0.85% of farmland, demonstrating that dual-use systems can reconcile energy and food production (Chatzipanagi et al., 2023). A California Central Valley study finds that replacing irrigated cropland with PV lowers food output but greatly improves farm cash flow, cuts regional water use by thousands of cubic meters annually, and delivers net revenues far exceeding lost crop income over the system's lifetime (Stid et al., 2025). Similarly, Giri and Mohanty (2026) evaluated the efficacy of a 0.675 kWp agrivoltaic configuration, which yielded 1115 kWh of energy and 21 kg of turmeric over 12 m^2. Despite the smaller footprint of the 7 m^2 open-field control (22 kg yield), the AVS demonstrated no significant deviations in plant morphology or phenology. These findings represent the first comprehensive techno-economic assessment of such systems, offering critical insights for the advancement of sustainable production and livelihood security at a national level.

Field-scale experiments have examined microclimatic conditions, water dynamics, electricity generation, and crop performance within AVS (e.g. Hassanpour Adeh et al., 2018; Marrou et al., 2013). Computational models have also been developed to simulate AVS functioning (Amaducci et al., 2018; Elamri et al., 2018). The outcomes of AVS (spanning energy production, crop growth and yield, and water availability and quality within the FEW nexus) are shaped by a range of critical variables. These include the configuration of solar PV arrays (panel inclination, azimuth orientation, height, and spacing), panel dimensions (length and width), and efficiency-related factors such as self-shading, operating temperature, dust accumulation, and snow cover. Additional influences arise from crop type, localized microclimatic conditions beneath and adjacent to panels (precipitation, wind, air temperature, solar radiation, and humidity), soil characteristics (moisture content, thermal properties, and chemical composition), and water use practices, including irrigation and panel cleaning.

Despite rapid progress in AVS research, existing modelling approaches have limited ability in representing the coupled food-water dynamics within AVS in three-dimensional space at the field scale. Current models often simplify spatial processes and do not fully capture the three-dimensional interactions between solar panel configuration, microclimate modification, and crop-water responses. This limitation restricts the ability to systematically evaluate how PV design parameters, such as panel azimuth, inclination, spacing, height, and dimensions, influence both agricultural productivity and water dynamics. For example, Elamri et al. (2018) developed the AVRAIN model to characterize the rain distribution in an agrivoltaic plot according to the tilting angles, heights, and sizes of solar PV panels. The predicted rain distribution in an agrivoltaic plot was then fed into HYDRUS-2D to investigate the effect of solar PV panels on water redistribution in shallow soils. However, (1) the rain distribution and water redistribution in shallow soils were simulated in two-dimensional (2D) space, which cannot represent the three-dimensional (3D) spatial differences in rain distribution, irrigation, and soil conditions in AVS; (2) it did not consider the impacts of other microclimatic conditions on water dynamics, such as solar radiation, snowfall, snowmelt (on the panel and on the ground), and solar panel cleaning using water; and (3) crop growth/yield was not included. Recent studies co-simulate crop growth and PV performance across various configurations to optimize dual-land use. However, significant challenges remain, including cross-climate validation, the high computational cost of high-resolution light modeling, and the absence of standardized protocols for coupling radiation, microclimate, and physiological crop models (Schuck et al., 2025; Zainali et al., 2025). For example, a study by Amaducci et al. (2018) created a radiation model to characterize solar energy distribution in AVS employing two-axis tracking technology; and the crop model GECROS was used to forecast maize yield and biomass in relation to weather conditions, soil water, and soil nitrogen utilizing information from every pixel. However, (1) it did not consider the impacts of other microclimatic conditions, such as rainfall, snowfall, snowmelt (on the panel and on the ground), and solar panel cleaning using water; and (2) it lacked the simulation of soil properties, water dynamics and crop growth in three-dimensional space.

Therefore, a field-scale model using an integrated framework that can capture the critical variables governing food and water dynamics in AVS in three-dimensional space is needed to support informed decision-making. The objectives of the paper were: (1) create a field-scale model (AVS-FW) using an integrated framework to represent the key factors focusing on food and water dynamics in AVS in three-dimensional space; and (2) demonstrate the AVS-FW by assessing the impacts of AVS on food and water dynamics, including the actual evapotranspiration, volumetric soil water content and amount of soil water stored at root depth, water flow, and lettuce yield (biomass) with and without solar PV panels.

In Objective 2, given the limited availability of field data, the AVS-FW model was applied at the experimental site through comparative scenario simulations (with and without PV panels) rather than direct validation against measured field data. The results highlighted additional data needs for future validation work. This section therefore focuses on demonstrating how the integrated framework used in the AVS-FW operates - showing process integration and system behavior under different AVS configurations. Therefore, model results were validated by comparing simulated trends and responses with findings reported in previous field-scale agrivoltaic studies.

The novelty of this study lies in establishing a field-scale model using an integrated framework that explicitly links microclimate redistributions, soil-water processes, and crop growth dynamics within AVS in three-dimensional space. Rather than focusing solely on model coupling, the framework provides a unified structure for analyzing spatial food-water interactions and evaluating AVS design scenarios. The integrated framework used in AVS-FW can provide decision-support for assessing alternative AVS layouts and supports the optimization of

AVS design toward sustainable development. By supporting improved land-use efficiency, water management, and renewable energy integration, this work contributes to sustainable development goals (SDG) related to zero hunger (SDG 2), clean water (SDG 6), and affordable and clean energy (SDG 7) created by the United Nations to guide sustainable development (UN, 2015).

2. Creation of the AVS-FW using an integrated framework to study the impacts of solar PV panels on food and water dynamics in three-dimensional space

2.1. An integrated framework for evaluating food and water dynamics in AVS in three-dimensional space

An integrated framework for evaluating food and water dynamics in AVS in three-dimensional space was created in this study (Fig. 1). This integrated framework allows simultaneous simulation of microclimate, soil-water process, and crop growth in AVS, providing comprehensive decision-support for evaluating tradeoffs among food production, water use, and solar energy generation. Such capability is critical for informing AVS design and policy decisions aimed at enhancing climate resilience, resource efficiency, and sustainable agricultural development. The primary components of the integrated framework in three-dimensional space include.

- **Local weather.** Local weather data (precipitation, solar radiation, humidity, wind, and temperature) are used to drive the field-scale simulation.
- **Solar PV panel.** The layouts (azimuth angles, inclinations, spacing, heights) and dimensions (lengths/widths) of solar PV panels for fixed systems (fixed azimuth angles and inclinations) or single/double axis tracking systems (changeable azimuth angles and/or inclinations) are needed to quantify the effects of the layouts and dimensions of solar PV panels. Solar panel cleaning using water needs to be represented to quantify how solar panel cleaning affects food and water dynamics. PV module parameters are needed to quantify the impacts of different solar panel features. Soil-plant-atmosphere-water-solar panel interactions are considered.
- **Microclimatic conditions under solar panels.** Microclimatic conditions under solar panels, including solar radiation, water depth (precipitation-rainfall and snowfall, melted snow-on the panel and on the ground, and solar panel cleaning water), humidity, wind, and temperature, are obtained in three-dimensional space to quantify soil-plant-atmosphere-water-solar panel interactions.
- **Soil condition and water transport.** By considering soil-plant-atmosphere-water-solar panel interactions, initial data for soil

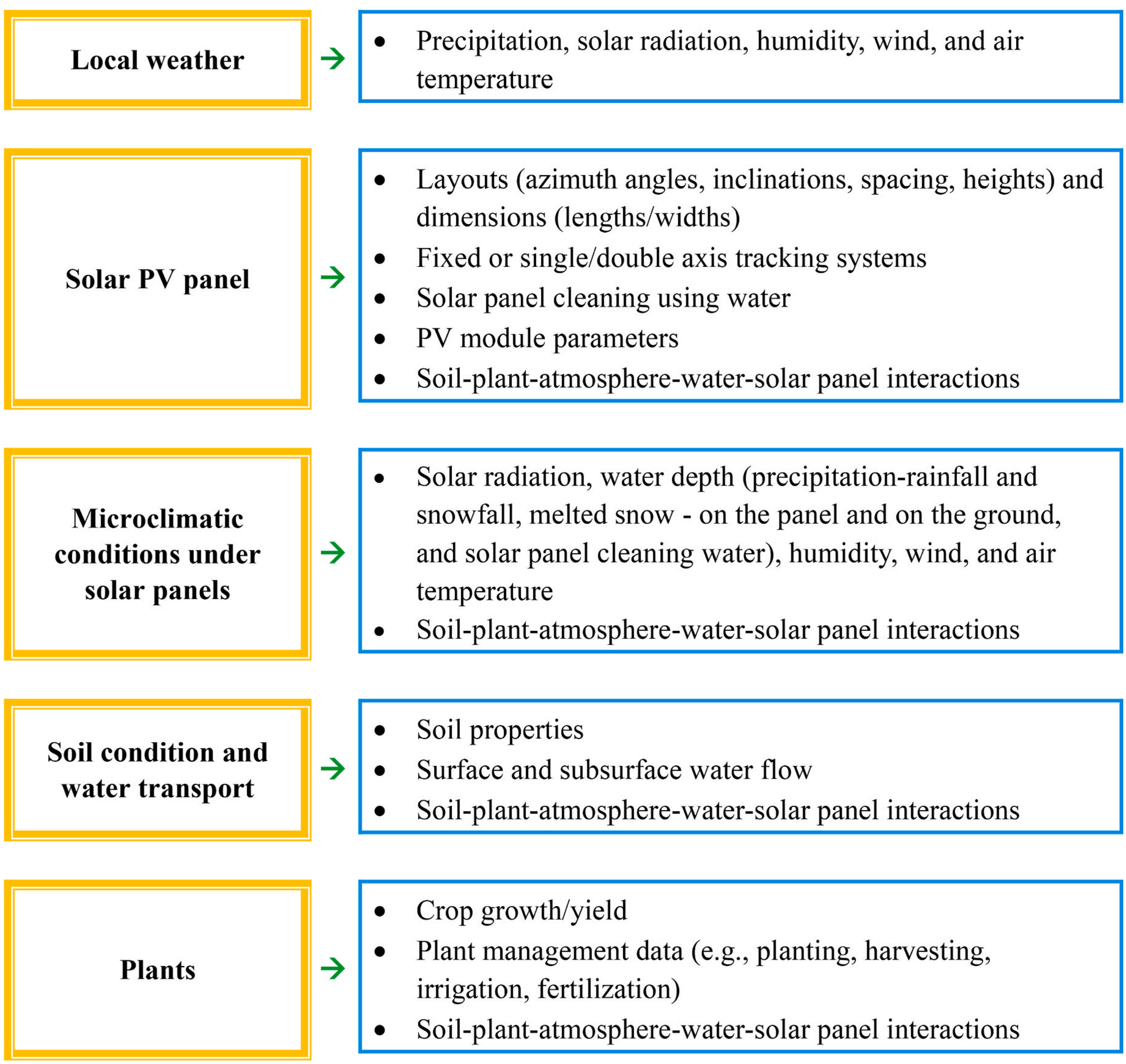

Fig. 1. An integrated framework for evaluating food and water dynamics in AVS in three-dimensional space.

properties in the field are needed and changes in soil properties over time can be simulated in three-dimensional space; and surface and subsurface water flow can be modeled in three-dimensional space.

- **Plant.** Plant growth/yield simulation using the microclimatic conditions under solar panels, integrated with plant management data (e.g., planting, harvesting, irrigation, fertilization) and soil-plant-atmosphere-water-solar panel interactions.

To demonstrate the application of the integrated framework for evaluating food and water dynamics in AVS in three-dimensional space, the AVS-FW model was developed using the integrated framework by dynamically integrating the AVS-Microclimate model (simulating three-dimensional microclimatic conditions under solar panels), R-SWMS model (simulating three-dimensional soil condition and water transport), and Soil and Water Assessment Tool (SWAT) crop growth module (simulating plant growth). The integrated framework used in AVS-FW adopts a modular integration strategy, coupling established models to represent microclimate, soil-water, and crop growth processes, thereby enabling flexible development while leveraging mature process formulations. The justifications for integrating these models/module are in the following sections.

Recent advances in AVS research have explored dynamic tracking PV systems, which aim to optimize solar energy capture while improving crop light conditions (i.e. Maddalena et al., 2025; Magadley et al., 2025). However, fixed (non-tracking) PV systems remain widely implemented in practice due to lower complexity and installation costs (Hammad et al., 2017); therefore, the AVS-FW model developed in present study focuses on modelling food-water dynamics under fixed-panel configurations, and future studies can be conducted to add solar tracking PV systems in the AVS-FW model.

2.2. The AVS-Microclimate model for simulating three-dimensional microclimatic conditions under solar panels

Microclimatic variations under solar panels (solar radiation, precipitation, air temperature, wind speed/direction, and relative humidity) are influenced by numerous factors, including canopy size and density/quantity, module array physical features (e.g., panel height, tilt angle, orientation, fixed-tilt or tracking system), and local climate. While solar panels can alter microclimatic conditions under solar panels such as air temperature, wind speed/direction, and relative humidity (Hassanpour Adeh et al., 2018), most studies indicated that those parameters change insignificantly under solar panels (Amaducci et al., 2018; Jing et al., 2022; Tahir and Butt, 2022). Based on majority of the findings in existing studies, solar radiation, precipitation (rainfall and snowfall), melted snow (on the panel/ground), and solar panel cleaning water under solar PV panels would vary greatly due to solar panels as obstacles; and air temperature, wind speed/direction, and relative humidity would be assumed to be unchanged when with and without solar panels. This simplification was adopted to isolate radiation-driven and water-driven effects on soil-plant-water dynamics. However, potential microclimatic variability represents a source of uncertainty that will be addressed in future model development.

The AVS-Microclimate model (Nguyen et al., 2026) has been created recently to quantify the three-dimensional redistributions of solar radiation and water depth (precipitation, melted snow, and solar panel cleaning water) under solar panels in AVS, which are critical for evaluating the food and water dynamics in AVS. The AVS-Microclimate model integrates multiple modules, including ground and solar panel positioning, solar radiation redistribution, snowfall and snowmelt, and the redistribution of precipitation, melted snow, and cleaning water from solar panels. By simulating these processes, AVS-Microclimate supports decision - making by evaluating how different solar PV panel configurations-such as inclination, azimuth angle, height, spacing, and dimensions (lengths/widths) - affect the redistributions of solar radiation and water depth beneath the panels, both of which are critical factors for crop production in AVS. Therefore, the AVS-Microclimate model (Nguyen et al., 2026) was selected for simulating three-dimensional microclimatic conditions under solar panels. The AVS-Microclimate model provided key input parameters for the current study, including redistributed solar radiation, rainfall, melted snow, and solar panel cleaning water on the ground.

2.3. The R-SWMS model for simulating three-dimensional soil condition and water transport

Numerical models have been developed to simulate solute transport and water flow in porous media, e.g., HYDRUS 1D/2D/3D and SWMS-3D (Simunek et al., 1995; Šimůnek et al., 2016). To simulate soil-plant-atmosphere-water-solar panel interactions in 3D space, an open-source 3D model is needed. A numerical model SWMS-3D (Simunek et al., 1995) simulates “the water and solute movement in unsaturated, partially saturated, or fully saturated porous media” in 3D space. But limitations exist in these models: (1) crop growth is not included; and (2) snowfall/snowmelt are not included.

In addition, a numerical model for simulating solute transport and water flow within the soil-plant system (R-SWMS) was developed by modifying the SWMS-3D model (open source) to couple with crop-growth or root-growth models (Javaux et al., 2008, 2013; Meunier et al., 2021). The methods in R-SWMS have been widely applied with significant strength in simulating soil water/solute transport; however, the crop growth module has not been fully completed. The R-SWMS model simulates water and solute movement in porous media by numerically solving the Richards' equation for water flow and the convection-dispersion equation for solute transport (Javaux et al., 2008; Simunek et al., 1995). The R-SWMS model (version 9.0 in 2008) integrated to the current AVS-FW model only includes the simulation of water flow. Therefore, the R-SWMS model was selected to simulate three-dimensional soil condition and water transport.

2.4. The SWAT crop growth module for simulating plant growth

The SWAT crop growth module, integrated in SWAT (Revision 685, released on September 6, 2022, was used in the current study), has been widely used with significant strengths in simulating plant growth (Li et al., 2021, 2024, 2025; Liu et al., 2019a; Liu et al., 2017, 2024; Ren et al., 2022; Li et al., 2026; Wu et al., 2026; Guo et al., 2022; Han et al., 2024; Liu et al., 2019b). The SWAT crop growth module (Neitsch et al., 2011) calculates potential crop growth and actual crop growth for all land covers (distinguishing between annual and perennial plants based on their growth cycles) considering factors such as yield prediction, heat unit, temperature thresholds, light interception, leaf area index, height of canopy, biomass, root growth, transpiration, water/nutrient uptake, water stress, temperature stress, and deficiencies in nutrients (e.g., nitrogen or phosphorus). The plant database of SWAT can be used for simulating different crop types. More details about the SWAT crop growth module are in Neitsch et al. (2011). Therefore, the SWAT crop growth module was selected for simulating crop growth.

Biomass production in the SWAT crop growth module is represented using process-based relationships linking intercepted radiation, transpiration, and plant growth processes. The calculation follows the SWAT crop growth module, where biomass accumulation is driven by radiation-use efficiency and water availability. A summary of the governing equations is provided in Eq. (1) (Neitsch et al., 2011).

$$\Delta \text{bio}_{\text{act},i} = \Delta \text{bio} \times \gamma_{\text{reg}} \quad \text{Eq. 1}$$

where $\Delta \text{bio}_{\text{act}}$ is the actual increase in total plant biomass on a given day i (kg/ha), Δbio is the potential increase in total plant biomass on a given day (kg/ha), and γ_{reg} is the plant growth factor (0.0 -1.0).

Detailed equations and input model parameters for biomass, leaf area index, water stress, and temperature stress are provided in the supplementary materials (Eq. S(1) to Eq. S(13), Eq. S(15)) (Neitsch et al., 2011). Evapotranspiration was calculated using the evapotranspiration module in SWAT model (Neitsch et al., 2011).

2.5. Soil-plant-atmosphere-water-solar panel interaction module

By integrating the AVS-Microclimate model (three-dimensional microclimatic conditions under solar panels), the R-SWMS model (three-dimensional soil condition and water transport), and SWAT crop growth module (plant growth), the soil-plant-atmosphere-water-solar panel interaction module in the AVS-FW model simulates water movement and plant growth in ground grids co-located with solar panels using the workflow with three main components (Fig. 2). The crop simulation process includes the following four steps.

Step 1: The model reads input data.

- Plant features in the plant database of the SWAT crop growth module
- Weather data: precipitation, solar radiation, air temperature, wind speed, relative humidity
- Irrigation depth applied for plant
- Soil property data for R-SWMS

Step 2: AVS-Microclimate calculates redistributed solar radiation and water depth under solar panels.

Step 3: AVS-FW model calculates parameters using Eq. (1) and Eq. S (1) to Eq. S(17) in the supplementary materials.

- Heat unit, light interception, potential leaf area index, potential evapotranspiration
- Soil pressure, soil water content, actual evapotranspiration
- Water stress, temperature stress, actual biomass, and actual leaf area index

Step 4: Provide crop growth output and water flow.

2.5.1. Read general data for all grids

General data for all grids are read: (i) Plant database for simulating

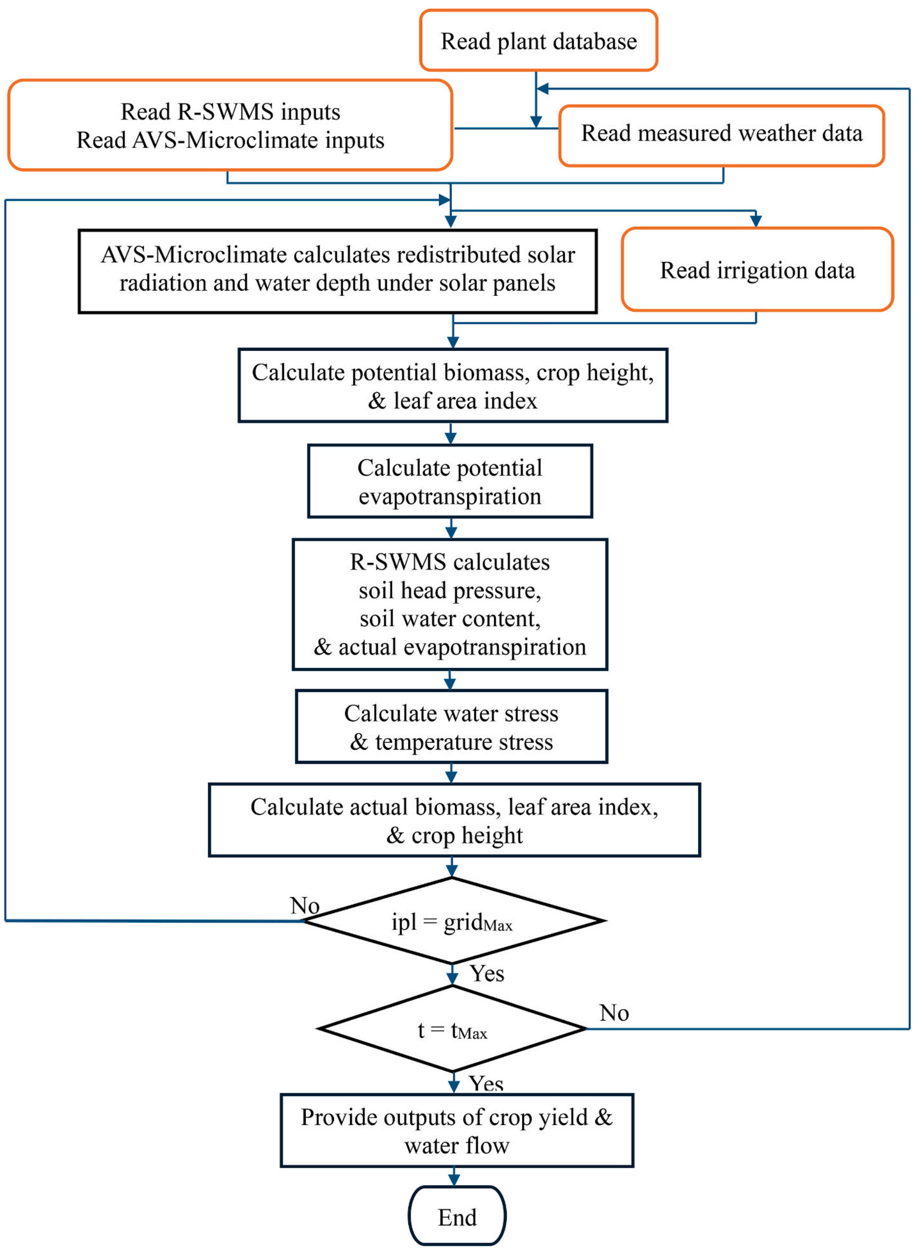

Fig. 2. Workflow of the soil-plant-atmosphere-water-solar panel interaction module.

plant growth in SWAT, which includes parameters such as plant code and name, maximum potential leaf area index, optimal temperature for plant growth, maximum root depth, maximum canopy height, and optimal temperature and minimum temperature for plant growth (Arnold et al., 2013). (ii) R-SWMS inputs, including field boundary, size of each grid, soil property, timestep, and boundary condition (Javaux et al., 2013). (iii) AVS-Microclimate inputs, including the layouts (inclinations, azimuth angles, heights, spacing) and sizes (lengths/widths) of solar PV panels; field location (latitude, longitude, elevation), inclination, azimuth angle, and boundary; and data of solar panel cleaning using water. (iv) Measured time series of weather data, including precipitation, solar radiation, air temperature, relative humidity, and wind speed/direction. (v) Irrigation data, including location, date/time, rate, and total volume.

2.5.2. Read the calculated data for each grid

Since the R-SWMS model reads data from each node, which represents the intersection of grid sides, we proposed a method to determine how data should be allocated to each node from the surrounding grid cells. For example (Fig. 3), for nodes (green text) located in the middle, data is calculated by averaging the values from the four surrounding cells (red text). For nodes on the boundaries, the data is calculated by averaging the values from the two adjacent cells. For nodes at the corners, the data is the value from the nearest cell. Therefore, the solar radiation and water depth reaching the ground grids simulated by the AVS-Microclimate model are allocated to nodes, and irrigation is applied for each node. The spatial averaging step is applied to enable consistent data transfer between grid-based and node-based model components. While this aggregation may smooth fine-scale spatial gradients, the approach is appropriate for capturing field-scale patterns targeted by the integrated framework used in AVS-FW. And by increasing the spatial resolution, the negative impacts of using this approach can be minimized in AVS simulation. However, this will lead to the tradeoff between computational feasibility and localized shadow-edge representation at the field scale.

2.5.3. Dynamically connect the inputs/outputs of different components

The inputs/outputs of the R-SWMS model, SWAT crop growth module, and AVS-Microclimate model are dynamically connected. After

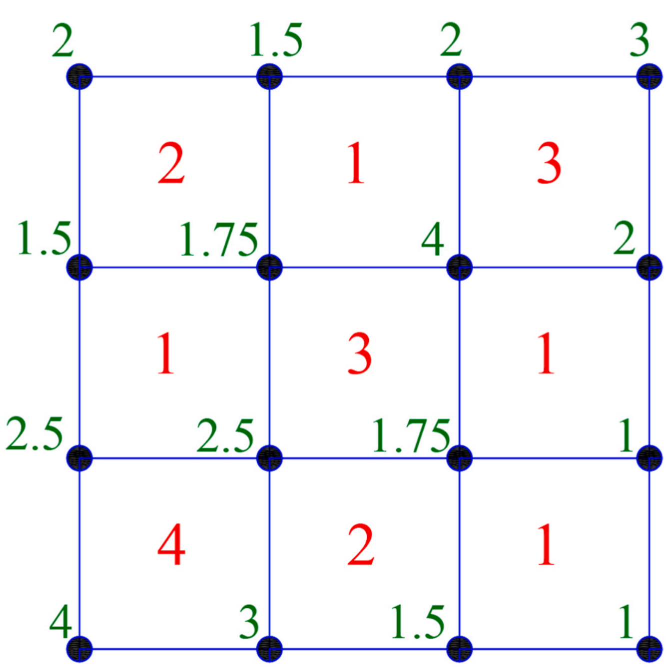

Fig. 3. Allocation of data to nodes from the surrounding grid cells.

reading the general data for all grids: (1) The AVS-Microclimate calculates redistributed solar radiation and water depth (precipitation-rainfall/snowfall, melted snow-on the panel/ground, and solar panel cleaning water) under solar panels. (2) The calculated data for each grid is read. (3) Potential biomass, crop height, and leaf area index for each grid are calculated. (4) Potential evapotranspiration is calculated. (5) Soil head pressure, soil water content, and actual evapotranspiration are computed. (6) Actual biomass, leaf area index, and crop height are calculated based on water stress and temperature stress. (7) The module loops all grids in each timestep until the end of the simulation period. (8) The final module outputs are crop yield and water flow.

The AVS-Microclimate model generates outputs at an hourly time step (e.g., solar radiation, rainfall, and melted snow), R-SWMS generates outputs at an hourly time step (e.g., soil, water), and the SWAT crop growth module operates at a daily time step. To ensure temporal consistency within the integrated framework, hourly outputs from AVS-Microclimate and R-SWMS are aggregated to daily values (e.g., daily totals or averages, depending on the variable) before being exchanged with the SWAT crop growth module.

3. Case study - demonstrate the application of the AVS-FW created using the framework

3.1. Study area and data availability

Colorado State University (CSU)'s Agricultural Research, Development, and Education Center–South (ARDEC South) was chosen as the study site for demonstrating the AVS-FW model. Beginning in 2018, CSU initiated a collaborative research program with Sandbox Solar of Fort Collins to experimentally evaluate how pole-mounted, small-scale PV arrays influence plant systems (Colorado Agrivoltaic Learning Center, 2018) (Fig. 4).

The modelling work in this study was based on an existing AVS case study which was carried out in 2020 and 2021 at ARDEC South (Uchanski et al., 2023). The research focused on a permanent experimental installation of pole-mounted PV arrays located on certified organic land. The PV panels were placed in an open field setting. The orientation of the arrays could be manually modified, ranging from a vertical position to a nearly horizontal position for field preparation. Each plot had drip irrigation installed with black plastic mulch (Fig. 4). Peppers, summer squash, lettuce, and tomatoes were the crop species examined in the experiment. The dataset derived from the ARDEC South experiments (Hickey, 2023; Solaredge, 2023; Uchanski et al., 2023), supplemented by additional external sources (CoAgMET, 2024; NASA, 2024), served as the basis for configuring and demonstrating the AVS-FW model (Table 1). A representative soil profile was applied across the domain to focus on evaluating the influence of AVS configuration on food-water dynamics. Potential effects of soil heterogeneity and localized compaction are acknowledged as recommendations for future work. In addition, the simulation period was aligned with the experimental lettuce growing season to evaluate food-water interactions. Assessment of off-season soil recharge and long-term hydrological impacts is beyond the present scope and represents an important direction for future research.

3.2. AVS-FW model setups and components in the AVS demonstrated

The layout of the case study site with one PV array (four solar PV panels) at ARDEC South was set up in the AVS-FW model to evaluate food and water dynamics in AVS by simulating soil-plant-atmosphere-water-solar panel interactions (Fig. 5). Lettuce was selected to demonstrate the AVS-FW model. For each growing season, the AVS-FW model was set up with one day for field preparation (June 1st) and one day for harvesting (September 30th). The nodes representing lettuce plants receiving irrigation water are highlighted with green circles (Fig. 5). The remaining nodes within the soil domain were modeled as bare soil,

Fig. 4. AVS experiments at the ARDEC South (Hickey, 2023).

Table 1
Data availability for the case study site at ARDEC South (Nguyen et al., 2026).

Type of data	Details
Data from the study at ARDEC South (Hickey, 2023; Solaredge, 2023; Uchanski et al., 2023)	
Location of the field	40.61° latitude and −104.99° longitude
Elevation of the field	1523 m
PV model	Jinko Solar's JKM325PP-72, 325W
PV material	Polycrystalline silicon (Opaque Si), 0% transparency
Size of solar panel	1956 mm × 992 mm × 41 mm
Operation inclination and facing	35°, face south
Height of the lower edge of PV array	1.22 m
Height of the upper edge of PV array	2.36 m
Soil	Nunn clay loam
Crop	Lettuce
Irrigation	Irrigation was applied three times per week through the drip irrigation lines in the north and south rows (Fig. 4). Each irrigation event was 3 h with the flow rate of 15 Lpm/30.5 m.
Size of area: Width × Length × Depth	60 m × 100 m × 1 m
Daily electricity generation of PV array from June 1, 2020 to September 30, 2022.	SolarEdge, The United States (Solaredge, 2023)
Data from other sources	
Hourly precipitation from June 1, 2020 to September 30, 2022.	NASA Center for Climate Simulation (NASA, 2024)
Other hourly climate data (air temperature, relative humidity, solar radiation, and wind speed) from June 1, 2020 to September 30, 2022.	CoAgMET, Colorado State University (CoAgMET, 2024)

indicating the absence of plants and irrigation.

The AVS-FW model was demonstrated by assessing the impacts of AVS on food and water dynamics, including the actual evapotranspiration, volumetric soil water content and amount of soil water stored at root depth, water flow, and lettuce yield (biomass) with and without solar PV panels. The growing season lasted 65 days from planting on June 30, 2020 (Hickey et al., 2024). Nodes in the north row (159, 161, 163, 165, 167) and nodes in the south row (237, 239, 241, 243, 245) were investigated (Fig. 5). The main differences between nodes in the north row and south row (Fig. 4) were: (i) nodes in the north row were at least partially shaded by the solar panels, while nodes in the south row were always in full sun condition; and (ii) precipitation, melted snow, and solar panel cleaning water redistribution were different at the nodes.

It should be noted that the application of the AVS-FW model in an experimental site conducted comparative scenario simulations (with and without PV panels) rather than direct validation against measured field data due to data limitations. The results revealed additional data that need to be collected in the future, providing future research directions for validation. Given the limited data available, this part of the paper aims to demonstrate the application of AVS-FW created using the integrated framework by showing how processes integrate and how the system behaves under different AVS configurations. Therefore, model results were validated by comparing simulated trends and responses with findings reported in previous field-scale agrivoltaic studies.

Regarding black plastic mulch as shown in Fig. 4, although it was used in the field experiment, mulch effects were not explicitly represented in the current setup. Consequently, soil evaporation was simulated without a dedicated mulch layer, which may influence water fluxes. This simplification is acknowledged as a modelling scope choice and will be addressed in future studies during model validation when experimental data are available. In addition, the selected grid resolution (0.5 m × 0.5 m) represents a balance between computational efficiency and representation of field-scale spatial variability within the field-scale model using the integrated framework. Finer spatial discretization may improve representation of localized irrigation and root uptake patterns, which is potential setups for future validation work when more observed data are available.

3.3. Impacts of lettuce moisture content differences in shaded and full sun areas on converting fresh weight to dry weight

Because lettuce moisture content was not measured during the field experiment while the model output would only have dry weight, a Monte Carlo-based sensitivity analysis (Doubilet et al., 1985 ; Yang, 2011) was conducted to evaluate the influence of plausible lettuce moisture-content differences between full-sun and shaded areas on converting fresh weight to dry weight. For the sensitivity analysis, the moisture content of the full-sun treatment was assigned a baseline value of 90% (Wang et al., 2021; J. Yang et al., 2024), whereas the moisture content of the shaded treatment was assumed to be 0 to 5% higher (ranging from 90% to 95%). These values were used to investigate the sensitivity of the fresh-to-dry weight conversion to plausible variations in plant water content rather than representing measured moisture contents. Two probability distributions of shaded vs. full sun moisture content differences were considered (Eq. (2)). The first employed a triangular distribution with a minimum of 0%, a most likely value of 1%, and a maximum of 5%, reflecting the expectation that small moisture-content differences were more likely than large ones. The second was a uniform distribution over the same range (0%-5%), assuming that all moisture-content differences had equal probability (Eq. (2)). For each probability distribution, 10,000 Monte Carlo realizations were generated.

For each realization, the shaded moisture content was randomly sampled from the selected probability distribution and converted to dry weight using Eq. (4) while dry weight in full sun was calculated using Eq. (3). The relative dry-weight difference between the shaded and full-sun treatments was subsequently calculated (Eq. (5)). The resulting distributions were analyzed using histograms and boxplots to quantify

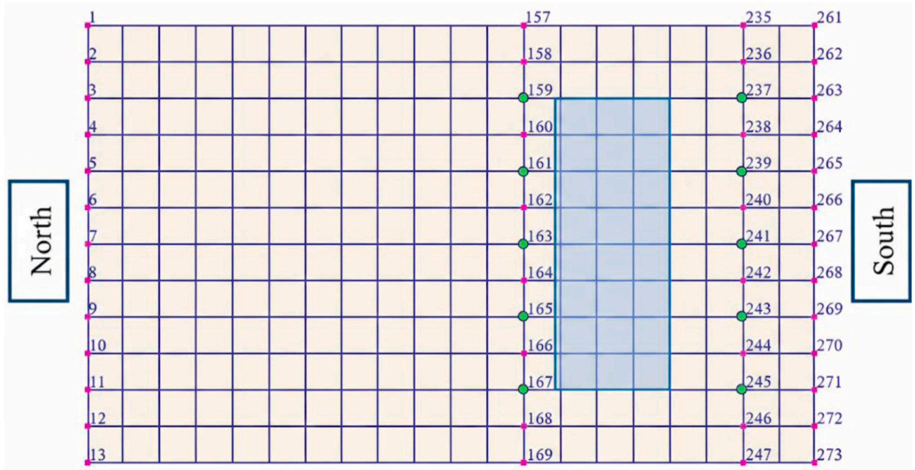

Fig. 5. Layout of the case study site at ARDEC South in the AVS-FW model to evaluate food and water dynamics by simulating soil-plant-atmosphere-water-solar panel interactions. Sizes of grids: 0.5 m × 0.5 m. Drip irrigation (green circle) at nodes 159, 161, 163, 165, 167 (north row) and 237, 239, 241, 243, 245 (south row) under the solar panels (blue rectangular) in the soil domain. (For interpretation of the references to colour in this figure legend, the reader is referred to the Web version of this article.)

the uncertainty associated with the fresh-to-dry weight conversion and to evaluate the robustness of the inferred dry-weight differences under alternative assumptions regarding moisture content.

$$M_{sh} = M_{fs} + \delta, \delta \sim \text{Triangular}(0, 1, 5) \quad \text{Or } M_{sh} = M_{fs} + \delta, \delta \sim \text{Uniform}(0, 5) \qquad \text{Eq. 2}$$

where M_{sh} is the moisture content of the shaded treatment (%), M_{fs} is the moisture content of the full-sun treatment (%), and δ represents the additional moisture content (%) in the shaded treatment, sampled from either a triangular or a uniform distribution.

$$DW_{fs} = FW_{fs}(1 - M_{fs}) \qquad \text{Eq. 3}$$

where DW_{fs} is the dry weight in the full sun treatment (g), FW_{fs} is the measured fresh weight in the full sun treatment (g), and M_{fs} is the moisture content in the full sun treatment (%).

$$DW_{sh} = FW_{sh}(1 - M_{sh}) \qquad \text{Eq. 4}$$

where DW_{sh} is the dry weight in the shaded treatment (g), FW_{sh} is the measured fresh weight in the shaded treatment (g), and M_{sh} is the moisture content in the shaded treatment (%).

$$\Delta = \frac{(DW_{sh} - DW_{fs})}{DW_{fs}} \times 100\% \qquad \text{Eq. 5}$$

where Δ is the relative dry-weight difference between full-sun and shaded treatments (negative values indicate lower dry weight under shade than in full sun), DW_{sh} is the dry weight in shaded treatment (g), and DW_{fs} is dry weight in full sun (g).

Table 2
The results of biomass, actual transpiration (epday), soil evaporation (esday), actual evapotranspiration (AET), amount of water stored at the root depth (solst), and volumetric soil water content (θ_w) for individual nodes. Biomass was the final values at the end of the lettuce growing period, while other results were the average values over the lettuce growing period.

Node ID	Biomass (ton/ha)	epday (mm)	esday (mm)	AET (mm)	solst (mm)	θ_w (cm^3/cm^3)
With solar panels						
159	13.377	1.546	3.378	4.924	20.290	0.272
161	11.021	1.408	2.884	4.291	21.007	0.278
163	10.171	1.358	2.716	4.074	21.317	0.281
165	10.996	1.407	2.879	4.286	21.019	0.278
167	13.402	1.547	3.342	4.890	20.174	0.271
237	17.577	1.792	4.167	5.959	18.855	0.259
239	17.408	1.782	4.163	5.945	18.960	0.260
241	17.383	1.781	4.159	5.940	18.962	0.261
243	17.407	1.782	4.168	5.950	18.969	0.261
245	17.573	1.792	4.148	5.939	18.837	0.259
Without solar panels (open field—before AVS project)						
159	18.041	1.819	4.256	6.074	18.725	0.260
161	18.041	1.819	4.296	6.115	18.805	0.260
163	18.041	1.819	4.299	6.118	18.810	0.260
165	18.041	1.819	4.296	6.115	18.805	0.260
167	18.041	1.819	4.256	6.074	18.725	0.260
237	18.041	1.819	4.244	6.062	18.702	0.259
239	18.041	1.819	4.290	6.109	18.792	0.260
241	18.041	1.819	4.293	6.112	18.799	0.260
243	18.041	1.819	4.290	6.109	18.792	0.260
245	18.041	1.819	4.244	6.062	18.702	0.259

4. Results and discussion

This section presents the results and discussion of actual evapotranspiration, volumetric soil water content and amount of soil water stored at root depth, water flow, and lettuce yield (biomass) with and without solar PV panels. The corresponding results for individual nodes are in Table 2.

4.1. Actual evapotranspiration (AET)

As in Table 2 and Fig. 6, the average AET over growing period at nodes 237-245 (south row with solar panels) was 32.35% higher than that of nodes 159-167 (north row with solar panels). Energy and water are needed to drive the evapotranspiration of water from leaves and soil. Solar panels can block direct sunlight, reducing the amount of solar energy reaching the ground; and solar panels can change the water distribution. Higher solar radiation and more available water in the south row compared to those of the north row were the key factors causing the higher rates of soil evaporation and lettuce transpiration. For example, the total solar radiation over growing season at node 241 (south row with solar panels, 2370.14 MJ/m^2) was 70.12% higher than that of node 163 (north row with solar panels, 1393.24 MJ/m^2); and the total water depth received (from irrigation and natural precipitation) over growing season by node 241 (south row with solar panels, 47.8 mm) was 7.17% higher than that of node 163 (north row with solar panels, 44.6 mm). The simulated decrease in AET from soil and lettuce in the area shaded by solar panels compared to that of unshaded area

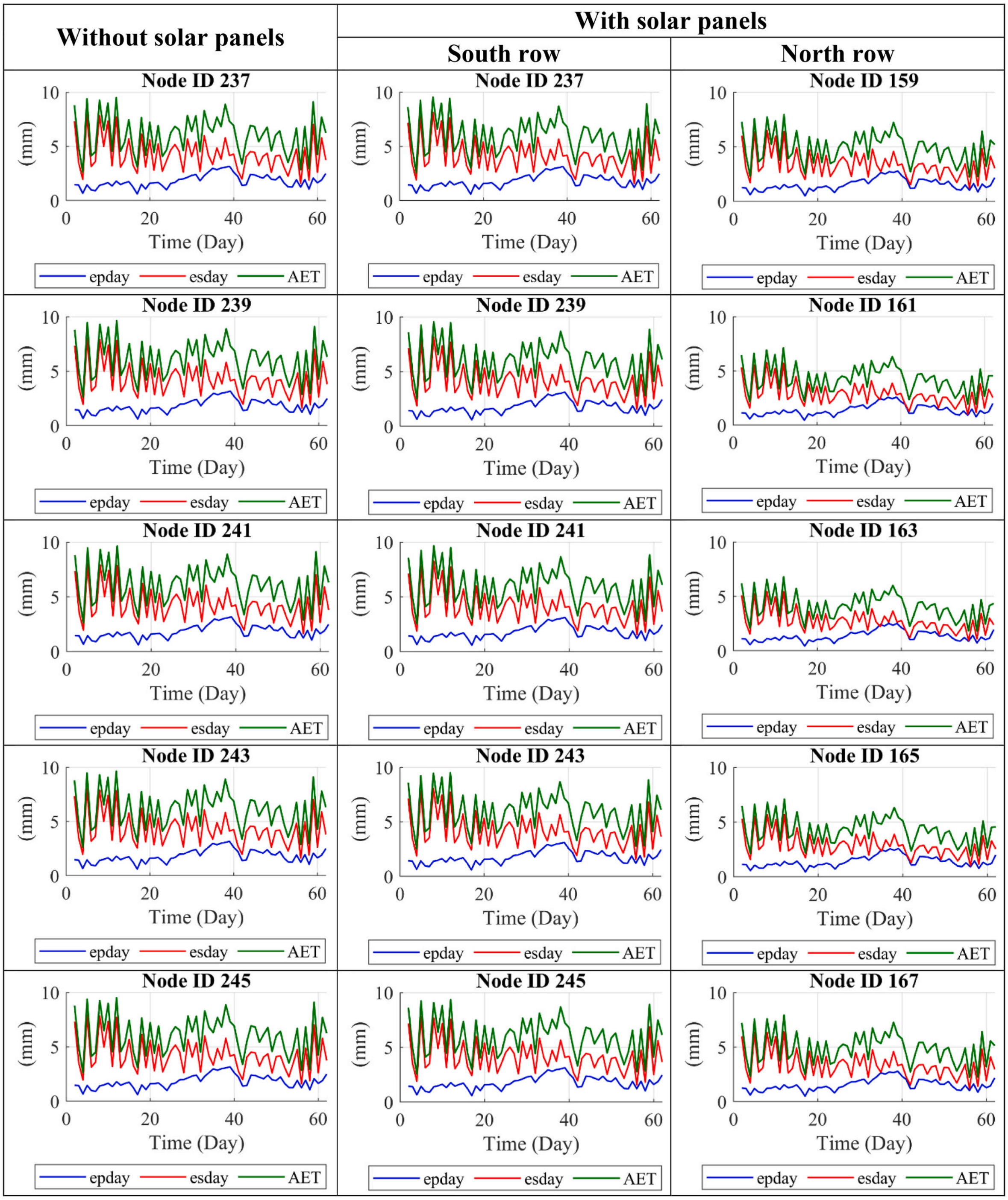

Fig. 6. Values of epday, esday, and AET at nodes 159, 161, 163, 165, 167, 237, 239, 241, 243, and 245 with and without solar panels, respectively.

aligned with the findings of Ali Abaker Omer et al. (2022).

Table 2 indicates that the AET values were very similar for nodes in the south row, around 5.947 mm/day; in the north row, the AET of the middle node (163) was about 16.97% lower compared to those of the edge nodes (159 and 167). In the north row, lettuce at the edge nodes (159 and 167) received partial direct solar radiation, more diffuse solar radiation, and higher water depth compared to those of the middle node (163), resulting in higher AET. In addition, compared to the AET of shaded middle node (163), the unshaded middle node (241) increased the AET by 45.80%. Compared to the AET of a shaded edge node (159), the corresponding unshaded edge node (237) increased the AET by 21.02%; while compared to the AET of the other shaded edge node (167), the corresponding unshaded edge node (245) increased the AET by 21.45%. These were caused by different solar radiation and water depth on the middle node and the edge nodes at two sides of the solar panels because of solar panel shading induced solar radiation redistribution and water redistribution.

Regarding the case without solar panels (open field condition), the corresponding nodes received the same amount of irrigation with lettuce grown (Table 2) while other nodes in the soil domain were treated as bare soil. The AET values of irrigated nodes for open field condition had high similarities (roughly 6.095 mm/day). Similar trends were found in the AET values over time at each node for both cases with and without solar panels (Fig. 6). The average AET over lettuce growing period with solar panels was 2.43% (south row) to 26.28% (north row) lower than without solar panels. The mean AET at Node 241, recorded at 5.94 mm/day, represents a marginal increase over the approximately 5.3 mm/day reported by Cabot et al. (2023) for the Upper Colorado Basin during the corresponding period. These could be caused by the differences in solar radiation, location, and water distribution for shaded and unshaded conditions (Marrou et al., 2013).

While the current AVS-Microclimate model focuses primarily on short-wave radiation redistribution and shading effects, PV panels may also emit long-wave thermal radiation due to panel heating. This additional heat flux could influence near-canopy microclimate and evapotranspiration processes. Under the climatic conditions of this case study, shading effects are expected to dominate energy balance changes. In addition, quantifying this contribution requires detailed thermal measurements and was beyond the scope of the present study. Future model development will consider inclusion of panel thermal radiation to further improve microclimate representation.

4.2. Volumetric soil water content and amount of soil water stored at root depth

The volumetric soil water content (θ_w) and amount of water stored at the root depth of 10 cm (solst) are in Table 2. The average volumetric soil water content of nodes in the south row with solar panels (0.260 cm^3/cm^3) was lower than that of nodes in the north row with solar panels (0.276 cm^3/cm^3) and slightly higher than that of nodes without solar panels (0.2598 cm^3/cm^3). In addition, the average amount of water stored at the root depth with solar panels was 0.80% (south row) to 10.63% (north row) higher than without solar panels (Table 2, Fig. 7). This was because the nodes in the south row with solar panels (237-245) received more water due to rainfall redistribution during rainy days caused by solar panels (Fig. S1), but these nodes also had significantly greater AET compared to those of nodes in the north row with solar panels (159-167). Compared to the condition without solar panels, the differences in volumetric soil water content and the amount of soil water stored at root depth for the south row and north row were also caused by the relative amount of water received and AET. This overall trend was consistent with previous research. Specifically, Hassanpour Adeh et al. (2018) concluded that the shade provided by solar panels reduced soil water depletion, leading to 15-25% greater soil moisture in the 10-60 cm root zone compared to areas without shade.

The three-dimensional nature of the AVS-FW model developed using the integrated framework refers to its numerical simulation capability, which represents spatial variability of microclimate and soil-water processes in three-dimensional space. In the present study, empirical soil moisture measurements at multiple horizontal positions and depths were not available. Therefore, the results presented were model outputs rather than direct field observations. Future studies can be conducted to obtain these measurements and provide additional data for model validation.

While the simulations suggest that PV panels can concentrate rainfall near drip edges and increase local water availability, such redistribution may also introduce potential risks. Localized water accumulation could negatively affect root aeration and respiration and may increase the risk

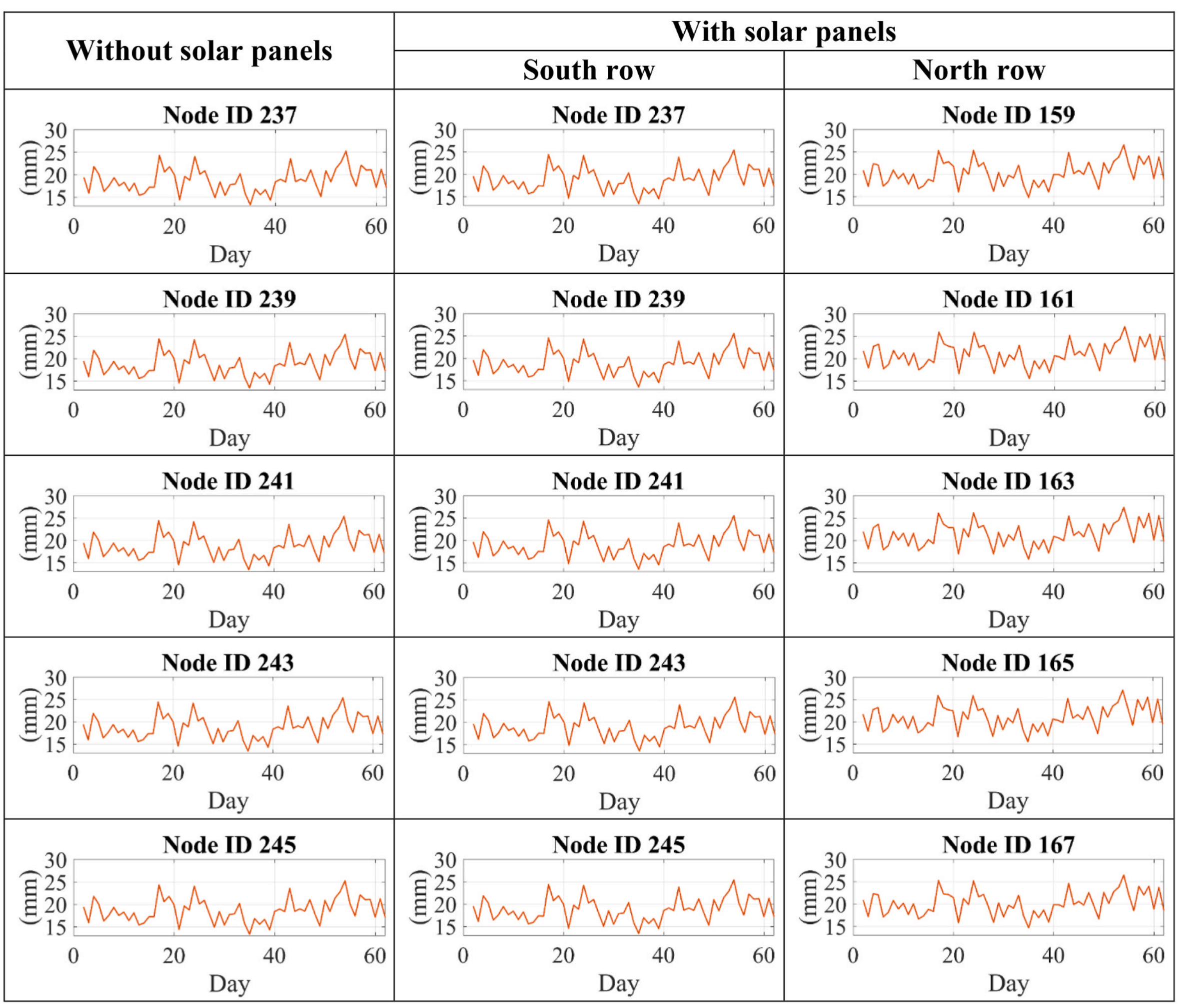

Fig. 7. The amount of water stored at root depth at nodes 159, 161, 163, 165, 167, 237, 239, 241, 243, and 245 with and without solar panels, respectively.

of nutrient leaching under certain soil and climatic conditions. The present study primarily focuses on evaluating changes in water availability and evapotranspiration dynamics; therefore, detailed assessment of biogeochemical processes such as root stress and nutrient transport was beyond its scope. Future studies should extend the AVS-FW model using the integrated framework to include these processes to better evaluate potential tradeoffs associated with localized water redistribution in AVS.

4.3. Water flow

The water flow for cases with and without solar panels was analyzed. Cumulative fluxes across the soil boundaries (wCumT) and total water volume in the soil domain (WatVol) were extracted to assess the water flow (Fig. 8) (Javaux et al., 2008). The wCumT accounts for the net water added or removed via boundary fluxes over the simulation period (e.g., rainfall, irrigation, evapotranspiration, and subsurface drainage). The bottom boundary of the soil domain was set to free drainage, meaning water exits the domain once the wetting front reaches the bottom. Negative values of wCumT indicate net inflow (more water entering the soil than leaving the soil), while positive values indicate net outflow (more water leaving the soil than entering the soil) (Javaux et al., 2008). A free-drainage lower boundary was applied to represent downward percolation in the absence of site-specific groundwater boundary information. Potential groundwater interactions were not represented and were acknowledged as an opportunity for future studies.

The patterns of wCumT over time for cases with and without solar panels were very similar but with varied magnitudes (Fig. 8a). These were also found for WatVol over time (Fig. 8b). For the cases with and without solar panels, the factors changed were rainfall/irrigation distribution and solar radiation distribution. Evapotranspiration was considered at irrigated nodes (159, 161, 163, 165, 167, 237, 239, 241, 243, and 245), while evaporation was considered for other nodes (simulated as bare soil); and all nodes were significantly impacted by solar radiation and water availability. It is important to note that soil evaporation and plant transpiration are significantly influenced by solar

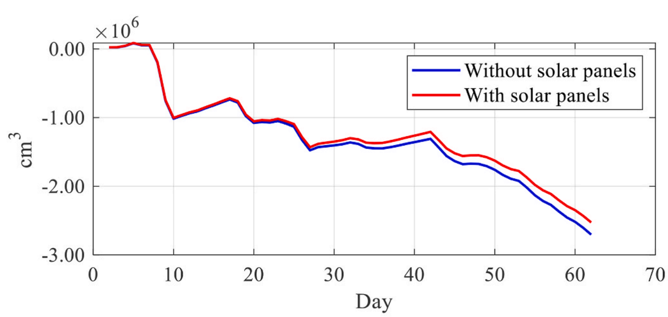

(a) Cumulative fluxes across the soil boundaries (wCumT)

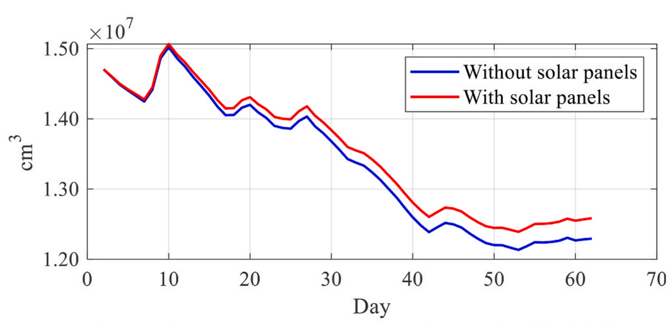

(b) Total water volume in the soil domain (WatVol)

Fig. 8. Cumulative fluxes across the soil boundaries (wCumT) and total water volume in the soil domain (WatVol) with and without solar panels.

radiation and available water (Hassanpour Adeh et al., 2018). Solar panels altered the spatial distribution of solar radiation, reduced the overall solar radiation on the soil domain, and altered the spatial distribution of water availability. The reduction in solar radiation can decrease evapotranspiration, leading to higher soil moisture content compared to conditions without solar panels. Consequently, WatVol values with solar panels were higher than those of without solar panels, particularly from day 30 to the end of the growing season, where the difference ranged from 159,000 cm^3/day to 291,000 cm^3/day (Fig. 8b). These indicate that the changes in the net water inflow/outflow through the domain boundaries caused by varied rainfall/irrigation distribution and solar radiation distribution for cases with and without solar panels were non-negligible.

For example, during the first 10 days, the wCumT in both cases (Fig. 8a) started at 0 cm^3, fluctuated slightly above 0 cm^3 first, and then dropped sharply to a negative value of -1×10^6 cm^3 as the soil surface received a large amount of water from irrigation and rainfall (Fig. S1) that gradually saturated the soil. The changes in wCumT led to a decrease in WatVol first, followed by a sharp increase in WatVol reaching over 1.5×10^7 cm^3. The rainfall and/or irrigation in this period added water to the top of the domain by infiltration. This water formed a wetting front that moved downward through the soil profile, as determined by Philip (1957). Based on the soil hydraulic properties of Nunn clay loam (Rawls et al., 1982) and a domain depth of 1 m, the wetting front could take several days to reach the bottom boundary with a free drainage condition (Simunek et al., 1995). Lettuce was in an early growth stage with shallow root depth; and the transpiration was minimal and evaporation changes were small during the period (Feddes, 1978). Similarly, the changes in wCumT and WatVol after day 10 were due to the relative balance of inflow (rainfall/irrigation) and outflow (evaporation, transpiration, and drainage) of the soil domain over time.

4.4. Lettuce yield (biomass)

Table 2 and Fig. S2 showed that the average biomass of lettuce (dry weight) at the end of the growing season with solar panels was 3.17% (south row) to 34.63% (north row) lower than without solar panels. In the north row with solar panels, the biomasses of lettuce at different nodes varied greatly; for example, the biomass of lettuce at the middle node (163) was 24.04% lower than that of the edge nodes (159 and 167). In the south row with solar panels, the biomasses of lettuce at all nodes were similar, while the biomasses of lettuce at nodes without solar panels were the same.

The results of the AVS-FW model were consistent with some previous findings, which concluded that shading can reduce lettuce yield by slowing down plant growth and limiting the accumulation of biomass at maturity (Asa'a et al., 2024; Marrou et al., 2013; Widmer et al., 2024; Zheng et al., 2021). Widmer et al. (2024) reported that in most experimental studies (11 out of 13), the lettuce grown under the panels had an average weight that was either significantly lower or only slightly higher compared to lettuce grown in full sun. While seasonal and varietal differences affected both fresh and dry weight, the dry weight was consistently lower for crops grown under the panels in those studies (Widmer et al., 2024). Similarly, according to Asa'a et al. (2024), when the shaded area under solar panels accounted for 30-40%, the highest dry mass of Malelona lettuce was recorded under full sun, followed by controlled tracking, solar tracking, and fixed modules in Montpellier, France. The Malelona lettuce exhibited an 18% decrease in dry mass within AVS, while the Kiribati variety showed no change. In another study, lettuce was grown under treatments in Hefei of Anhui, China under natural state, conventional agrivoltaic system (CAS), and even-lighting agrivoltaic system (EAS) (Zheng et al., 2021). CAS markedly reduced lettuce performance, with fresh and dry weight decreases of 53.5% and 60.5%, respectively, compared to the natural state, alongside slower growth and poorer morphology. Conversely, EAS maintained yields statistically similar to open-field conditions, supporting normal growth and acceptable quality.

In contrast, other studies found relatively higher lettuce yields in shaded areas compared to unshaded conditions (Amaro de Sales et al., 2021; Ilić et al., 2017; Semchenko et al., 2012). Whether lettuce yield is higher or lower in shaded versus unshaded conditions is determined by several factors. These include the season (spring or summer), location, varietal, temperature, and the solar panel arrangement, which affect the light conditions (full sun, moderate shade, or heavy shade; light quality and intensity) (Amaro de Sales et al., 2021; Widmer et al., 2024). Regarding light quality and intensity, F. Zhang et al. (2023) tested lettuce yield under a large-scale SCAPV (Spectral-separated Concentrated Agrivoltaics) system in Anhui, China. Lettuce showed a 47.9% gain compared to open-air cultivation. Under open-air conditions, summer overheating reduced lettuce yields, while under SCAPV, growth remained normal due to moderate temperature and better microclimate condition. Generally, shade-tolerant species (e.g., lettuce) can maintain moderate growth under moderately shaded conditions, despite light limitations. However, a significant reduction in lettuce yield would be observed when the shade level is too high.

The substantial difference in simulated dry weight biomass between north and south rows can be attributed to several factors. In SWAT, dry weight biomass accumulation is primarily driven by solar radiation, leaf area index, radiation-use efficiency, and water and temperature stresses (Eq. S(10), Eq. S(14)). Consequently, as shading reduces sunlight availability (the other parameters are kept constant), biomass accumulation is directly proportional to the incident solar radiation. The simulated results from the case study revealed a 41.2% difference in solar radiation between the north and south rows over the simulation period (section 4.1). This led to the large reduction in the simulated dry weight biomass of lettuce in shaded areas.

For more accurate results, crop yield calibration should be conducted using experimental data. SWAT default crop growth module assumes light-demanding plants; therefore, the radiation-use efficiency (RUE) of shade-tolerant crops should be simulated more realistically (Hao et al., 2022). The improved radiation interception efficiency (RIE) for the lettuce in the shaded area was also highlighted in Marrou et al. (2013), which found biomass reduction was less than the reduction in available light in almost all cases. This means lettuce can use light more efficiently to produce biomass in the condition of less available light. Additionally, shaded-adapted crops typically exhibit thinner leaves, wider canopies, and more efficient light capture due to reduced energy waste (Asa'a et al., 2024; Sanchez et al., 1989). Consequently, the maximum leaf area index could be a crucial parameter for calibration. Furthermore, since irrigation ensured water was not a stressor for lettuce growth in this study, parameters related to temperature stress (Neitsch et al., 2011) such as the base temperature (below which plant growth ceases) and optimum temperature (the ideal temperature for growth) should also be modified. Given the complexity of the plant response to light and microclimate, the crop module within the AVS-FW model is limited by the latest advances in crop physiology and crop-water-climate interactions. It is also limited by developments in crop-specific yield models and plant-scale data-intensive inputs and calibrations.

The AVS-FW model represents light availability primarily through irradiance intensity and does not explicitly account for changes in light spectral composition under PV panels with diffuse/direct light. However, PV structures may alter the spectral distribution of incoming radiation, which can influence plant physiological responses, photosynthetic efficiency, and crop morphology. As a result, omission of light quality effects may introduce uncertainty in crop growth predictions, particularly for species that are sensitive to spectral variations. Incorporating spectral light modelling into future versions of the AVS-FW using the integrated framework could improve representation of crop responses and further enhance prediction accuracy.

Although the present study was demonstrated using a single case study site in Colorado and lettuce as a representative crop, the primary objective was to develop and evaluate a field-scale model using an integrated modelling framework rather than establishing universally applicable crop responses. Because lettuce is generally considered shade-tolerant, the magnitude of biomass and evapotranspiration responses observed here may differ for crops with higher light sensitivity. Future improvements of the AVS-FW using the integrated framework will require calibration using more comprehensive experimental datasets as they become available and may incorporate advanced crop growth models, such as AquaCrop, to enhance crop yield estimation. Developed by the Food and Agriculture Organization (FAO), AquaCrop is a dynamic crop model that simulates canopy development, crop transpiration, biomass accumulation, and final yield (Vanuytrecht et al., 2014), offering potential for improved representation of crop-specific responses within AVS environments. In addition, although reductions in crop biomass were observed under certain AVS configurations, overall AVS performance should be evaluated by considering both agricultural yield and PV energy generation. Metrics such as Land Equivalent Ratio (LER) require integrated assessment of food and energy outputs; therefore, while this study focuses on food-water dynamics and crop responses, complementary to studies addressing energy yield analysis. Future work will combine these components to enable full system-level evaluation of AVS efficiency and economic viability.

4.5. Model validation discussion

Validation of AVS at the field scale remains a significant challenge due to the limited availability of comprehensive experimental datasets that simultaneously capture soil-plant-atmosphere-water interactions under PV structures. Findings from one climate, crop, panel height, spacing, or shading setup do not transfer cleanly to another. This limitation is widely acknowledged in recent agrivoltaic research (Mahim et al., 2026; Weselek et al., 2019). In this study, validation is therefore addressed through a multi-level approach to ensure the credibility and robustness of the proposed AVS-FW, as indicated in Vander Heyden et al. (2001).

First, the reliability of the AVS-FW is supported by the established performance of its core components. The SWAT model has been extensively validated in hydrological and agroecosystem studies across a wide range of climatic and soil conditions (Neitsch et al., 2011). Similarly, the R-SWMS model has been widely applied and validated for simulating three-dimensional soil water flow and root water uptake processes. By integrating these well-established models, the AVS-FW builds upon scientifically validated foundations (Javaux et al., 2008).

Second, a component-level validation strategy is adopted. Individual processes simulated within the model-such as soil moisture dynamics, evapotranspiration, and crop growth-are evaluated against expected ranges and behaviors reported in the literature. The simulated outputs demonstrate physically consistent responses to key agrivoltaic drivers. These responses are consistent with previously reported findings in AVS, supporting the internal validity of the model. As shown in Table 3, the simulated dry-weight reduction in the current study (34.63%) falls within the range reported in previous studies (23% to 88%) based on dry-weight biomass indicators, with an average reported yield reduction of approximately 46.5%. Regarding experimental data in the case study, the available ARDEC South dataset reported lettuce fresh weight, while the AVS-FW model simulated dry biomass. Because fresh weight includes plant water content, whereas dry biomass reflects accumulated structural biomass, these variables are not directly equivalent (Hortamericas, 2021). Under agrivoltaic conditions, reduced radiation may lower dry matter accumulation, while reduced evapotranspiration and moderated microclimate, radiation interception efficiency may maintain plant fresh weight (Ali Abaker Omer et al., 2022; Marrou et al., 2013; Zou et al., 2025). Therefore, the observed non-significant difference in fresh weight at ARDEC South (Hickey et al., 2024) cannot be directly used to validate the simulated dry biomass response without a conversion factor or paired fresh/dry measurements.

Table 3
Comparison of lettuce biomass reduction under agrivoltaic conditions between the current study and previous studies.

No.	Current and previous studies	Reduction in lettuce dry weight (%) under solar panels compared to full sun conditions	Dry weight or fresh weight biomass
1	Current study	34.63%	Dry weight
2	Asa'a et al. (2024)	30-40%	Dry weight
3	Zheng et al. (2021)	60.5%	Dry weight
4	Zou et al. (2025)	23.7-27.9%	Dry weight
5	Marrou et al. (2013)	55-88%	Dry weight
6	Hickey et al. (2024) - ARDEC SOUTH [a]	No significant difference in fresh weight (about −5.7%)	Fresh weight

[a] This paper describes the experimental results of a case study, which served as the foundation for the current research.

Third, sensitivity analysis was conducted to assess the uncertainty of converting fresh weight to dry weight due to lettuce moisture content differences in shaded and full sun areas (section 3.3). The experimental dataset (Hickey et al., 2024) reported lettuce yield as fresh weight (105 g/head in full sun and 111 g/head under solar panels), whereas the simulation model predicts dry biomass. Consequently, a conversion from fresh weight to dry weight is required to enable comparison between experimental observations and the simulated results. Fresh weight comprises both plant dry matter and water, and can therefore vary substantially with plant water status (Wang et al., 2021). Moisture content represents the proportion of water in fresh plant tissue and is commonly expressed as a percentage of fresh weight. Previous studies have shown that lettuce contains a high proportion of water typically around 90%, while environmental conditions can influence plant water status and consequently the relationship between fresh and dry weights (Wang et al., 2021; J. Yang et al., 2024). Agrivoltaic shading modifies the light environment and affects physiological processes such as photosynthesis, stomatal conductance, and transpiration, all of which are closely associated with plant water relations (Jamil et al., 2025). Therefore, although fresh weight may remain nearly unchanged, differences in moisture content may result in different dry matter accumulation. This uncertainty should be considered when converting fresh weight to dry weight. Fig. 9 shows that the estimated dry-weight difference between shaded and full-sun treatments was generally negative under both moisture-content assumptions, indicating lower dry matter accumulation in the shaded treatment. Under the triangular distribution (Fig. 9a), the dry weight differences had a mean of −15.40%, a minimum-to-maximum range of −47.01% to 5.66%, and a lower quartile to higher quartile range of −23.48% to −6.19%; whereas the uniform distribution (Fig. 9b) produced a mean of −20.80%, a minimum-to-maximum range of −47.14% to 5.71%, and a lower quartile to higher quartile range of −33.95% to −7.54%. The boxplots further (Fig. 9c) confirmed that both the mean and median were negative for each distribution, while the uniform distribution showed greater spread, indicating higher uncertainty. Overall, the results suggest that the slightly greater fresh weight observed under shading compared to full sun was likely attributable to higher lettuce moisture content rather than greater dry matter. The simulated dry-weight reduction of 34.63% was within the uncertainty range estimated by the moisture-content sensitivity analysis, indicating that the modeled yield reduction is plausible under reasonable assumptions of higher moisture content in the shaded treatment.

Finally, the present study explicitly identifies the key parameters governing system behavior, including soil properties and crop growth parameters. This provides a clear pathway for future calibration and validation as more field-scale datasets for AVS become available. The proposed model is therefore positioned as a foundational tool that enables systematic integration of processes and supports progressive refinement through future empirical studies.

While full system-level validation remains constrained by data

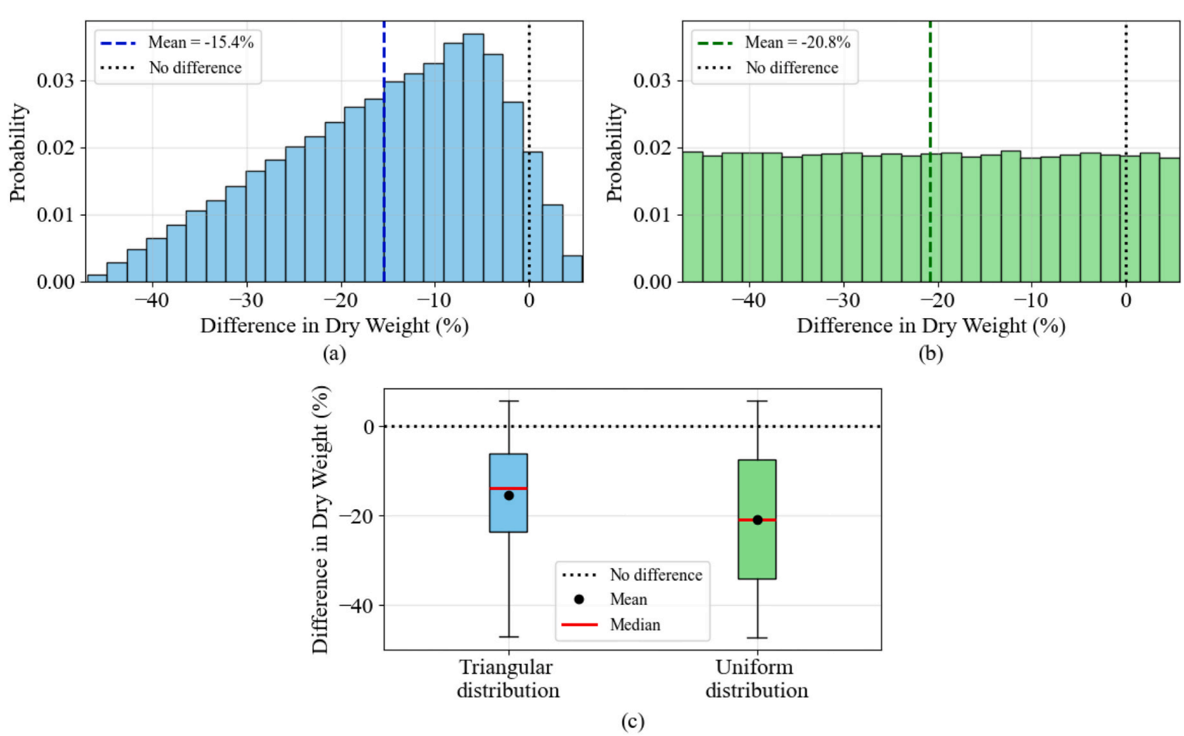

Fig. 9. Sensitivity analysis - impacts of lettuce moisture content differences in shaded vs. full sun areas (triangular and uniform distributions) on converting fresh weight to dry weight. (a) Histogram of percent dry weight changes under triangular distribution. (b) Histogram of percent dry weight changes under uniform distribution. (c) Boxplot of percent dry weight changes under triangular and uniform distributions. Negative values indicate lower dry weight in the shaded treatment than in the full-sun treatment.

availability, the multi-level validation approach adopted in this study enhances the credibility of the AVS-FW model and demonstrates its capability to realistically represent coupled food-water dynamics in AVS.

5. Conclusions

This study developed a field-scale model (AVS-FW) using an integrated framework to simulate three-dimensional food and water dynamics in AVS by coupling microclimate, soil-water, and crop growth processes. Application of the AVS-FW to a case study site in Colorado demonstrated that PV panels can substantially influence evapotranspiration, soil water storage, water fluxes, and crop biomass, emphasizing the importance of spatially explicit representation of soil-plant-atmosphere-water-solar panel interactions in AVS environments. Compared with existing approaches, the AVS-FW created using the integrated framework enables integrated evaluation of PV layout and design parameters, providing a practical tool for assessing tradeoffs between crop production and water dynamics in AVS design.

The novelty of this study lies in establishing a field-scale model using an integrated framework that explicitly links microclimate redistributions, soil-water processes, and crop growth dynamics within AVS in three-dimensional space. Rather than focusing solely on model coupling, the integrated framework provides a unified structure for analyzing spatial food-water interactions and evaluating AVS design scenarios.

The results revealed additional data that need to be collected in the future, providing future research directions for validation. Although model evaluation was constrained by limited experimental data and optimization of specific management configurations was beyond the scope of this study, the framework of the AVS-FW model establishes a foundation for future calibration, validation, and scenario-based management analysis as additional field measurements become available. From a practical perspective, the framework of AVS-FW can support farmers and land managers in evaluating how different AVS configurations influence crop performance and water availability under site-specific conditions. This enables informed decision-making to balance potential yield reductions with water conservation benefits. In addition, the framework can support scenario analysis and decision support for AVS design, irrigation management, and climate adaptation strategies. Overall, the framework of AVS-FW supports improved AVS planning and contributes to more sustainable land use and resource management within the Food-Energy-Water nexus.

CRediT authorship contribution statement

Anh H. Nguyen: Formal analysis, Investigation, Methodology, Software, Validation, Visualization, Writing – original draft. **Yaoze Liu:** Conceptualization, Funding acquisition, Investigation, Methodology, Project administration, Resources, Software, Supervision, Writing – review & editing. **Siyu Li:** Formal analysis, Software, Writing – review & editing. **Zhuohang Wu:** Formal analysis, Software, Writing – review & editing. **Majdi R. Abou Najm:** Methodology, Writing – review & editing. **Liming Zhou:** Methodology, Writing – review & editing. **Xiaobo Xue Romeiko:** Methodology, Writing – review & editing. **Richard R. Perez:** Methodology, Writing – review & editing. **Mark E. Uchanski:** Methodology, Writing – review & editing. **Jennifer M. Bousselot:** Methodology, Writing – review & editing. **Hu Liu:** Methodology, Writing – review & editing. **Chuandong Wu:** Conceptualization, Methodology, Writing – review & editing.

Declaration of competing interest

The authors declare that they have no known competing financial interests or personal relationships that could have appeared to influence the work reported in this paper.

Acknowledgements

The authors would like to thank Thomas Hickey for his contribution to the experimental data.

Appendix A. Supplementary data

Supplementary data to this article can be found online at https://doi.org/10.1016/j.jclepro.2026.148908.

Data availability

Data will be made available on request.

References

Ali Abaker Omer, A., Liu, W., Li, M., Zheng, J., Zhang, F., Zhang, X., Ingenhoff, J., 2022. Water evaporation reduction by the agrivoltaic systems development. Sol. Energy 247, 13–23. https://doi.org/10.1016/j.solener.2022.10.022.

Amaducci, S., Yin, X., Colauzzi, M., 2018. Agrivoltaic systems to optimise land use for electric energy production. Appl. Energy 220, 545–561. https://doi.org/10.1016/j.apenergy.2018.03.081.

Amaro de Sales, R., Chaves de Oliveira, E., Buzatto, E., Ferreira de Almeida, R., Alves de Lima, M.J., da Silva Berilli, S., Cunha Siman, F., 2021. Photo-selective shading screens as a cover for production of purple lettuce. Sci. Rep. 11 (1), 14972. https://doi.org/10.1038/s41598-021-94437-5.

Arnold, J.G., Kiniry, J.R., Srinivasan, R., Williams, J.R., Haney, E.B., Neitsch, S.L., 2013. SWAT 2012 input/output Documentation. Retrieved from.

Asa'a, S., Reher, T., Rongé, J., Diels, J., Poortmans, J., Radhakrishnan, H.S., Daenen, M., 2024. A multidisciplinary view on agrivoltaics: future of energy and agriculture. Renew. Sustain. Energy Rev. 200, 114515.

Cabot, P.E., Hipps, L.E., Schroeder, M., Derwingson, A.R., 2023. Estimation of Actual Evapotranspiration Using Eddy Covariance. Retrieved from Kremmling, CO: https://www.coloradobasinroundtable.org/wp-content/uploads/2023/11/Technical-Memo-2022-Evaluating-Conserved-Consumptive-Use-Upper-Colorado-Eddy-Covariance.pdf.

Campana, P.E., Stridh, B., Amaducci, S., Colauzzi, M., 2021. Optimisation of vertically mounted agrivoltaic systems. J. Clean. Prod. 325, 129091. https://doi.org/10.1016/j.jclepro.2021.129091.

Chatzipanagi, A., Taylor, N., Jaeger-Waldau, A., 2023. Overview of the Potential and Challenges for agri-photovoltaics in the European Union. Publications Office of the European Union, Luxembourg, 132879.

CoAgMET, 2024. Colorado Agricultural Meteorological Network (Coagmet). Retrieved from. https://coagmet.colostate.edu.

Colorado Agrivoltaic Learning Center, 2018. Agrivoltaics 101. https://www.coagrivoltaic.org/agrivoltaics-101.

Doubilet, P., Begg, C.B., Weinstein, M.C., Braun, P., McNeil, B.J., 1985. Probabilistic sensitivity analysis using Monte Carlo simulation: a practical approach. Med. Decis. Mak. 5 (2), 157–177.

Elamri, Y., Cheviron, B., Mange, A., Dejean, C., Liron, F., Belaud, G., 2018. Rain concentration and sheltering effect of solar panels on cultivated plots. Hydrol. Earth Syst. Sci. 22 (2), 1285–1298. https://doi.org/10.5194/hess-22-1285-2018.

FAO, 2021. Make every drop of water count. https://www.fao.org/newsroom/detail/make-every-drop-of-water-count/en?utm.

Feddes, R., 1978. 4.3 Simulation of Field Water Use and Crop Yield.

Gadhiya, G., Patel, U., Chauhan, P., Giri, N.C., Yin, G.-Z., Khargotra, R., 2024. Development of agrivoltaic insect net house to enhance sustainable energy-food production: a techno-economic assessment. Results Eng. 24, 103228. https://doi.org/10.1016/j.rineng.2024.103228.

Giri, N.C., Mohanty, R.C., 2026. Turmeric crop farming potential under Agrivoltaic system over open field practice in Odisha, India. Environ. Dev. Sustain. 28 (2), 2663–2681. https://doi.org/10.1007/s10668-024-05086-3.

Guo, T., Liu, Y., Shao, G., Engel, B., Sharma, A., Marshall, L., Flanagan, D., Cibin, R., Wallace, C., Zhao, K., Ren, D., Vera Mercado, J., Aboelnour, M., 2022. Improving probabilistic monthly water quantity and quality predictions using a simplified residual-based modeling approach. Environ. Model. Software 156, 105499. https://doi.org/10.1016/j.envsoft.2022.105499.

Hammad, B., Al-Sardeah, A., Al-Abed, M., Nijmeh, S., Al-Ghandoor, A., 2017. Performance and economic comparison of fixed and tracking photovoltaic systems in Jordan. Renew. Sustain. Energy Rev. 80, 827–839. https://doi.org/10.1016/j.rser.2017.05.241.

Han, J., Xin, Z., Shan, G., Liu, Y., Xu, B., Zhang, Q., Zhang, C., 2024. Developing nutrient pollution management strategies on a watershed scale under climate change. Ecol. Indic. 159, 111691. https://doi.org/10.1016/j.ecolind.2024.111691.

Hao, K., Liu, X., Wang, X., Fei, L., Liu, L., Jie, F., Shan, Y., 2022. Optimizing Shade Cultivation Method and Irrigation Amount to Improve Photosynthetic Characteristics, Bean Yield, and Quality of Coffee in a Subtropical Monsoon Climate, vol. 13. https://doi.org/10.3389/fpls.2022.848524, 2022.

Hassanpour Adeh, E., Selker, J.S., Higgins, C.W., 2018. Remarkable agrivoltaic influence on soil moisture, micrometeorology and water-use efficiency. PLoS One 13 (11), e0203256.

Hickey, T., 2023. Plant Growth Under Photovoltaic Arrays of Varying Transparencies–A Study of Plant Response to Light and Shadow in Agrivoltaic Systems.
Hickey, T., Uchanski, M., Bousselot, J., 2024. Vegetable crop growth under photovoltaic (PV) modules of varying transparencies. Heliyon 10 (16), e36058. https://doi.org/10.1016/j.heliyon.2024.e36058.
Hortamericas, 2021. Fresh weight vs. dry weight. https://hortamericas.com/blog/fresh-weight-vs-dry-weight/#more-27823.
IEA, 2025. Global Energy Review 2025 - Electricity. Retrieved from. https://www.iea.org/reports/global-energy-review-2025/electricity.
Ilić, S.Z., Milenković, L., Dimitrijević, A., Stanojević, L., Cvetković, D., Kevrešan, Ž., Mastilović, J., 2017. Light modification by color nets improve quality of lettuce from summer production. Sci. Hortic. 226, 389–397. https://doi.org/10.1016/j.scienta.2017.09.009.
Šimůnek, J., Van Genuchten, M.T., Šejna, M., 2016. Recent developments and applications of the HYDRUS computer software packages. Vadose Zone J. 15 (7).
IRENA, 2025. Record-Breaking annual growth in renewable power capacity. https://www.irena.org/News/pressreleases/2025/Mar/Record-Breaking-Annual-Growth-in-Renewable-Power-Capacity?utm.
Jamil, U., Rahman, M.M., Hayibo, K.S., Alrayes, L., Fordjour, E., Thomas, R., Pearce, J. M., 2025. Transparency effects in agrivoltaics lettuce cultivation using uniform/non-uniform semitransparent photovoltaic modules in controlled environments. Sol. Energy 302, 114006. https://doi.org/10.1016/j.solener.2025.114006.
Javaux, M., Couvreur, V., Vanderborght, J., Vereecken, H., 2013. Root water uptake: from three-dimensional biophysical processes to macroscopic modeling approaches. Vadose Zone J. 12 (4) vzj2013-2002.
Javaux, M., Schröder, T., Vanderborght, J., Vereecken, H., 2008. Use of a three-dimensional detailed modeling approach for predicting root water uptake. Vadose Zone J. 7 (3), 1079–1088. https://doi.org/10.2136/vzj2007.0115.
Jing, R., Liu, J., Zhang, H., Zhong, F., Liu, Y., Lin, J., 2022. Unlock the hidden potential of urban rooftop agrivoltaics energy-food-nexus. Energy 256, 124626.
Li, S., Liu, Y., Her, Y., Chen, J., Guo, T., Shao, G., 2021. Improvement of simulating sub-daily hydrological impacts of rainwater harvesting for landscape irrigation with rain barrels/cisterns in the SWAT model. Sci. Total Environ. 798, 149336. https://doi.org/10.1016/j.scitotenv.2021.149336.
Li, S., Liu, Y., Her, Y., Nguyen, A.H., 2024. Enhancing the SWAT model for creating efficient rainwater harvesting and reuse strategies to improve water resources management. J. Environ. Manag. 366, 121829.
Li, S., Liu, Y., Nguyen, A.H., Wu, Z., Al-Farsi, M.Z., Choi, T., Ren, D., 2025. A framework for creating sustainable rainwater harvesting and reuse strategies for urban landscape irrigation in a changing climate. J. Environ. Manag. 392, 126852.
Li, Y., Ren, D., Engel, B., Liu, Y., Hu, M., Li, J., Huang, G., 2026. Process-based simulation of the water-food-energy-environment nexus in a photovoltaic and drip irrigation planned agricultural district. Agric. Water Manag. 329, 110357. https://doi.org/10.1016/j.agwat.2026.110357.
Liu, Y., Guo, T., Wang, R., Engel, B.A., Flanagan, D.C., Li, S., Wallace, C.W., 2019a. A SWAT-based optimization tool for obtaining cost-effective strategies for agricultural conservation practice implementation at watershed scales. Sci. Total Environ. 691, 685–696.
Liu, Y., Li, S., Nguyen, A.H., Engel, B.A., Chen, J., Flanagan, D.C., Liu, C., 2024. An integrated tool for cost-effectively applying nutrient management practices for corn, soybeans, and wheat. Sci. Total Environ. 955, 177110.
Liu, Y., Li, S., Wallace, C.W., Chaubey, I., Flanagan, D.C., Theller, L.O., Engel, B.A., 2017. Comparison of computer models for estimating hydrology and water quality in an agricultural watershed. Water Resour. Manag. https://doi.org/10.1007/s11269-017-1691-9.
Liu, Y., Wang, R., Guo, T., Engel, B.A., Flanagan, D.C., Lee, J.G., Wallace, C.W., 2019b. Evaluating efficiencies and cost-effectiveness of best management practices in improving agricultural water quality using integrated SWAT and cost evaluation tool. J. Hydrol. 577, 123965.
Maddalena, B., Leonhard, J.G., Matthew, F.B., 2025. Enhancing agrivoltaic synergies through optimized tracking strategies. J. Photon. Energy 15 (3), 032703. https://doi.org/10.1117/1.JPE.15.032703.
Magadley, E., Matar, M., Kabha, R., Korabi, R., Hajyahya, A., Abasi, A., Yehia, I., 2025. The electrical performance of a single-axis sun tracking agrivoltaic system inside a polytunnel greenhouse. Energy Convers. Manag. X 26, 100940. https://doi.org/10.1016/j.ecmx.2025.100940.
Mahim, T.M., Rahman, M.M., Huda, A.S.N., 2026. Review of the challenges and prospects in agrivoltaics. Adv. Energy Sustain. Res. 7 (1), e202500227.
Marrou, H., Wery, J., Dufour, L., Dupraz, C., 2013. Productivity and radiation use efficiency of lettuces grown in the partial shade of photovoltaic panels. Eur. J. Agron. 44, 54–66. https://doi.org/10.1016/j.eja.2012.08.003.
Meunier, F., Couvreur, V., Draye, X., Lobet, G., Huber, K., Schroeder, N., Schnepf, A., 2021. Investigating soil–root interactions with the numerical model R-SWMS. In: Plant Systems Biology: Methods and Protocols. Springer, pp. 259–283.
NASA, 2024. NASA Center for Climate Simulation Hourly Precipitation Data.
Neitsch, S.L., Williams, J.R., Arnold, J.G., Kiniry, J.R., 2011. Soil and Water Assessment Tool Theoretical Documentation—Version 2009. Texas Water Resources Institute, College Station.
Nguyen, A., Cochrane, T., Pahlow, M., 2022. Optimising water allocation and land management to mitigate the effects of land use and climate change on reservoir performance. Hydrol. Sci. J. https://doi.org/10.1080/02626667.2022.2132162.
Nguyen, A.H., Liu, Y., Li, S., Wu, Z., Abou Najm, M.R., Zhou, L., Wu, C., 2026. A field-scale model for simulating the redistribution of solar radiation and water on the ground surface under solar panels in agrivoltaic systems. Renew. Energy 273, 126108. https://doi.org/10.1016/j.renene.2026.126108.
Pekk, L., Varbanov, P.S., Pan, T., Weltsch, Z., Radli-Burjan, B., Hary, A., Wang, X.-C., 2025. Future of Agrivoltaic projects: a review from the technological forecasting perspective. Clean. Eng. Technol. 28, 101057. https://doi.org/10.1016/j.clet.2025.101057.
Philip, J.R., 1957. The theory of infiltration: 1. The infiltration equation and its solution. Soil Sci. 83 (5), 345–358.
Pourshafi, P., Maixner, A., Bakhtiari, A., Hanifi, H., 2025. Performance analysis of a novel photovoltaic module design for vertical applications: mitigate self-shading of bifacial modules. Renew. Energy, 124186.
Rawls, W.J., Brakensiek, D.L., Saxtonn, K.E., 1982. Estimation of soil water properties. Transactions of the ASAE 25 (5), 1316–1320.
Ren, D., Engel, B., Mercado, J.A.V., Guo, T., Liu, Y., Huang, G., 2022. Modeling and assessing water and nutrient balances in a tile-drained agricultural watershed in the US Corn Belt. Water Res., 117976
Sanchez, C.A., Allen, R.J., Schaffer, B., 1989. Growth and yield of crisphead lettuce under various shade conditions. J. Am. Soc. Hortic. Sci. 114 (6), 884–890.
Schuck, F., Bach, H., Bousi, E., Schindele, S., 2025. Agrivoltaics crop yield modeling: quantifying the effects of light limitations on crop growth. AgriVoltaics Conference Proceedings 3. https://doi.org/10.52825/agripv.v3i.1361.
Semchenko, M., Lepik, M., Götzenberger, L., Zobel, K., 2012. Positive effect of shade on plant growth: amelioration of stress or active regulation of growth rate? J. Ecol. 100 (2), 459–466. https://doi.org/10.1111/j.1365-2745.2011.01936.x.
Simunek, J., Huang, K., Van Genuchten, M.T., 1995. The SWMS_3D Code for Simulating Water Flow and Solute Transport in three-dimensional variably-saturated Media, vol. 139. US Salinity Laboratory Agricultural Research Service.
Solaredge, 2023. SolarEdge: solar powering people's lives around the USA. https://monitoringpublic.solaredge.com/solaredge-web/p/site/.
Stid, J.T., Shukla, S., Kendall, A.D., Anctil, A., Hyndman, D.W., Rapp, J., Anex, R.P., 2025. Impacts of agrisolar co-location on the food–energy–water nexus and economic security. Nat. Sustain. 8 (6), 702–713. https://doi.org/10.1038/s41893-025-01546-4.
Tahir, Z., Butt, N.Z., 2022. Implications of spatial-temporal shading in agrivoltaics under fixed tilt & tracking bifacial photovoltaic panels. Renew. Energy 190, 167–176.
Turnley, J.W., Grant, A., Schull, V.Z., Cammarano, D., Sesmero, J., Agrawal, R., 2024. The viability of photovoltaics on agricultural land: can PV solve the food vs fuel debate? J. Clean. Prod. 469, 143191.
Uchanski, M., Hickey, T., Bousselot, J., Barth, K.L., 2023. Characterization of agrivoltaic crop environment conditions using opaque and thin-film semi-transparent modules. Energies 16 (7). https://doi.org/10.3390/en16073012.
UN, 2015. Transforming our world: the 2030 Agenda for sustainable development. https://sdgs.un.org/2030agenda.
Vander Heyden, Y., Nijhuis, A., Smeyers-Verbeke, J., Vandeginste, B.G.M., Massart, D.L., 2001. Guidance for robustness/ruggedness tests in method validation. J. Pharmaceut. Biomed. Anal. 24 (5), 723–753. https://doi.org/10.1016/S0731-7085(00)00529-X.
Vanuytrecht, E., Raes, D., Steduto, P., Hsiao, T.C., Fereres, E., Heng, L.K., Mejias Moreno, P., 2014. AquaCrop: fao's crop water productivity and yield response model. Environ. Model. Software 62, 351–360. https://doi.org/10.1016/j.envsoft.2014.08.005.
Varo-Martínez, M., López-Bernal, A., De Ahumada, L.F., López-Luque, R., Villalobos, F.J., 2024. Simulation model for electrical and agricultural productivity of an olive hedgerow Agrivoltaic system. J. Clean. Prod. 477, 143888.
Wang, W., Ma, Y., Fu, L., Cui, Y., Majeed, Y., 2021. Physical and mechanical properties of hydroponic lettuce for automatic harvesting. Inf. Process. Agric. 8 (4), 550–559. https://doi.org/10.1016/j.inpa.2020.11.005.
Weselek, A., Ehmann, A., Zikeli, S., Lewandowski, I., Schindele, S., Högy, P., 2019. Agrophotovoltaic systems: applications, challenges, and opportunities. A review. Agron. Sustain. Dev. 39 (4), 35. https://doi.org/10.1007/s13593-019-0581-3.
Widmer, J., Christ, B., Grenz, J., Norgrove, L., 2024. Agrivoltaics, a promising new tool for electricity and food production: a systematic review. Renew. Sustain. Energy Rev. 192, 114277.
Wu, Z., Li, S., Liu, Y., Mattoon, E., Al-Farsi, M., Her, Y., Chen, J., Feng, X., Jaber, F., 2026. Improvement of simulating rain gardens to advance sustainable stormwater management. J. Environ. Manag. 401, 128853. https://doi.org/10.1016/j.jenvman.2026.128853.
Yang, J., 2011. Convergence and uncertainty analyses in Monte-Carlo based sensitivity analysis. Environ. Model. Software 26 (4), 444–457. https://doi.org/10.1016/j.envsoft.2010.10.007.
Yang, J., Song, J., Liu, J., Dong, X., Zhang, H., Jeong, B.R., 2024. Prolonged post-harvest preservation in lettuce (Lactuca sativa L.) by reducing water loss rate and chlorophyll degradation regulated through lighting direction-induced morphophysiological improvements. Plants 13 (18). https://doi.org/10.3390/plants13182564.
Zainali, S., Lu, S.M., Fernández-Solas, Á., Cruz-Escabias, A., Fernández, E.F., Zidane, T.E. K., Campana, P.E., 2025. Modelling, simulation, and optimisation of agrivoltaic systems: a comprehensive review. Appl. Energy 386, 125558. https://doi.org/10.1016/j.apenergy.2025.125558.
Zhang, F., Li, M., Zhang, W., Liu, W., Omer, A.A.A., Zhang, Z., Zhang, X., 2023. Large-scale and cost-efficient agrivoltaics system by spectral separation. iScience 26 (11).

Zhang, L., Gong, J., Yang, Z., Wu, X., Wang, W., Yang, C., Bao, E., 2025. Evaluating the contribution of decreasing heights of photovoltaic panels on light environment and agricultural production in agrivoltaic systems. J. Clean. Prod. 495, 145091.

Zheng, J., Meng, S., Zhang, X., Zhao, H., Ning, X., Chen, F., Liu, W., 2021. Increasing the comprehensive economic benefits of farmland with even-lighting Agrivoltaic Systems. PLoS One 16 (7), e0254482. https://doi.org/10.1371/journal.pone.0254482.

Zou, J., Luo, S., Shi, M., Wang, D., Liu, W., Shen, Y., Jiang, Y., 2025. Effects of different light intensities on lettuce growth, yield, and energy consumption optimization under uniform lighting conditions. PeerJ 13, e19229. https://doi.org/10.7717/peerj.19229.